New Standard for the Logarithmic Accuracy of Parton Showers

Melissa van Beekveld,[1] Mrinal Dasgupta,[2] Basem Kamal El-Menoufi,[3] Silvia Ferrario Ravasio,[4] Keith Hamilton,[5] Jack Helliwell,[6] Alexander Karlberg,[4] Pier Francesco Monni,[4] Gavin P. Salam,[6,7] Ludovic Scyboz,[3] Alba Soto-Ontoso,[4] and Gregory Soyez[8]

[1]*Nikhef, Theory Group, Science Park 105, 1098 XG Amsterdam, The Netherlands*
[2]*Department of Physics & Astronomy, University of Manchester, Manchester M13 9PL, United Kingdom*
[3]*School of Physics and Astronomy, Monash University, Wellington Rd, Clayton VIC-3800, Australia*
[4]*CERN, Theoretical Physics Department, CH-1211 Geneva 23, Switzerland*
[5]*Department of Physics and Astronomy, University College London, London WC1E 6BT, United Kingdom*
[6]*Rudolf Peierls Centre for Theoretical Physics, Clarendon Laboratory, Parks Road, Oxford OX1 3PU, United Kingdom*
[7]*All Souls College, Oxford OX1 4AL, United Kingdom*
[8]*IPhT, Université Paris-Saclay, CNRS UMR 3681, CEA Saclay, F-91191 Gif-sur-Yvette, France*

(Received 14 June 2024; revised 10 October 2024; accepted 5 December 2024; published 3 January 2025)

We report on a major milestone in the construction of logarithmically accurate final-state parton showers, achieving next-to-next-to-leading-logarithmic (NNLL) accuracy for the wide class of observables known as event shapes. The key to this advance lies in the identification of the relation between critical NNLL analytic resummation ingredients and their parton-shower counterparts. Our analytic discussion is supplemented with numerical tests of the logarithmic accuracy of three shower variants for more than a dozen distinct event-shape observables in $Z \to q\bar{q}$ and Higgs $\to gg$ decays. The NNLL terms are phenomenologically sizeable, as illustrated in comparisons to data.

DOI: 10.1103/PhysRevLett.134.011901

Parton showers are essential tools for predicting QCD physics at colliders across a wide range of momenta from the TeV down to the GeV regime [1–4]. In the presence of such disparate momenta, the perturbative expansions of quantum field theories have coefficients enhanced by large logarithms of the ratios of momentum scales. One way of viewing parton showers is as automated and immensely flexible tools for resumming those logarithms, thus correctly reproducing the corresponding physics.

The accuracy of resummations is usually classified based on terms with the greatest logarithmic power at each order in the strong coupling (leading logarithms or LL), and then towers of terms with subleading powers of logarithms at each order in the coupling (next-to-leading logarithms or NLL, NNLL, etc.). Higher logarithmic accuracy for parton showers should make them considerably more powerful tools for analyzing and interpreting experimental data at CERN's Large Hadron Collider and potential future colliders. The past years have seen major breakthroughs in advancing the logarithmic accuracy of parton showers, with several groups taking color-dipole showers from LL to NLL [5–18]. There has also been extensive work on incorporating higher-order splitting kernels into showers [19–29] and understanding the structure of subleading-color corrections, see e.g. Refs. [6,30–41].

Here, for the first time, we show how to construct parton showers with NNLL accuracy for the broad class of event-shape observables at lepton colliders, like the well-known Thrust [42,43] (see, e.g., Refs. [44–65] for calculations at NNLL and beyond). This is achieved by developing a novel framework that unifies several recent developments, on (a) the inclusive structure of soft-collinear gluon emission [58,66] up to third order in the strong coupling α_s; (b) the inclusive pattern of energetic ("hard") collinear radiation up to order α_s^2 [67,68]; and (c) the incorporation of soft radiation fully differentially up to order α_s^2 in parton showers, ensuring correct generation of any number of well-separated pairs of soft emissions [29]. These are all NNLL after integration of the respective (a) double and (b), (c) single logarithmic phase spaces.

We will focus the discussion on the $e^+e^- \to Z \to q\bar{q}$ process, with the understanding that the same arguments apply also to $H \to gg$. Each event has a set of emissions with momenta $\{k_i\}$ and we work in units where the centre-of-mass energy $Q \equiv 1$. We will examine the probability $\Sigma(v)$ that some global event shape, $V(\{k_i\})$, has a value $V(\{k_i\}) < v$. Event-shape observables have the property [69] that for a single soft and collinear emission k, $V(k) \propto k_t e^{-\beta_{\rm obs}|y|}$, where k_t (y) is the transverse momentum (rapidity) of k with respect to the Born event direction and

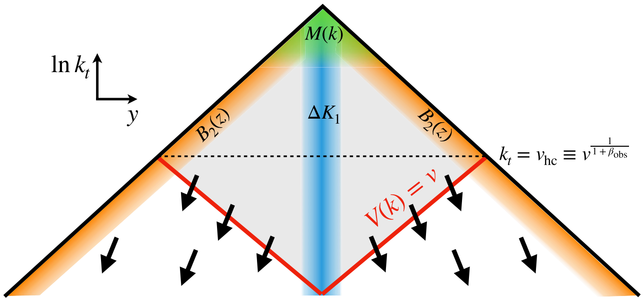

FIG. 1. Schematic representation of the Lund plane [70]. A constraint on an event shape that scales as $k_t e^{-\beta_{\mathrm{obs}}|y|}$ implies that shower emissions above the red line are mostly vetoed. At NNLL, one mechanism that modifies this constraint is that subsequent branching may cause the effective transverse momentum or rapidity to shift, as represented by the arrows.

β_{obs} depends on the specific observable, e.g., $\beta_{\mathrm{obs}} = 1$ for Thrust. Whether considering analytic resummation or a parton shower, for $v \ll 1$ we have

$$\Sigma(v) = \mathcal{F} \exp\left[-4 \int \frac{dk_t}{k_t} \int_{k_t}^{1} dz P_{gq}(z) M(k) \times \frac{\alpha_{\mathrm{eff}}}{2\pi} \Theta(V(k) > v)\right], \tag{1}$$

with $P_{gq}(z) = C_F\{[1 + (1 - z)^2]/z\}$ and $M(k)$ a function that accounts for next-to-leading order matching, with $M(k) \to 1$ for $k_t \to 0$. The exponential is a Sudakov form factor, encoding the suppression of emissions with $V(k) > v$, cf. the gray region of Fig. 1. It brings the LL contributions to $\ln \Sigma$, terms $\alpha_s^n L^{n+1}$ with $L = \ln v$, as well as NLL ($\alpha_s^n L^n$), NNLL ($\alpha_s^n L^{n-1}$), etc., contributions. The function $\mathcal{F}$ accounts [69] for the difference between the actual condition $V(\{k_i\}) < v$ and the simplified single-emission boundary $V(k) < v$ that is used in the Sudakov. It starts at NLL.

In Eq. (1), the effective coupling, α_{eff}, can be understood as the intensity of gluon emission, inclusive over possible subsequent branchings of that emission and corresponding virtual corrections. We write it as

$$\alpha_{\mathrm{eff}} = \alpha_s \left[1 + \frac{\alpha_s}{2\pi}(K_1 + \Delta K_1(y) + B_2(z)) + \frac{\alpha_s^2}{4\pi^2} K_2\right], \tag{2}$$

with $\alpha_s \equiv \alpha_s^{\overline{\mathrm{MS}}}(k_t)$ and here the rapidity $y = \ln z/k_t$. $K_1 = [(67/18) - (\pi^2/6)]C_A - (10/9)n_f T_R$ (often called K_{CMW}) [71] is required for NLL accuracy and the remaining terms for NNLL. $\Delta K_1(y)$ is zero in the resummation literature, nonzero at central rapidities for certain showers, and vanishes for $y \to \infty$ [29]; $B_2(z)$ affects the hard-collinear region and tends to zero in the soft limit, $z \to 0$. In analytic resummation it is generally included as a constant multiplying $\delta(1 - z)$ [44]. It has been calculated in specific resummation schemes in Refs. [67,68], but is not yet known for the showers that we consider, which also do not yet include the relevant triple-collinear dynamics. At NNLL, K_2 is relevant in the whole soft-collinear region and also so far calculated only for analytic resummation [58,66]. Through shower unitarity, α_{eff} is relevant also in the Sudakov-veto region of Fig. 1, i.e., the region above the red line, even though that region contains no emissions or subsequent branching.

It is straightforward to see from Eq. (1) that terms up to $\alpha_s^n L^{n-1}$ in $\ln \Sigma(v)$ depend only on the integrals of $\Delta K_1(y)$ and $B_2(z)$,

$$\Delta K_1^{\mathrm{int}} \equiv \int_{-\infty}^{\infty} dy \Delta K_1(y), \quad B_2^{\mathrm{int}} \equiv \int_0^1 dz \frac{P_{gq}(z)}{2C_F} B_2(z). \tag{3}$$

One of the key observations of this Letter is that as long as a parton shower correctly generates double-soft emissions in the soft-collinear region (as required for NNLL handling of event shape sensitivity to multiple emissions), it is then possible and sufficient to identify NNLL relations between the $\Delta K_1^{\mathrm{int}}$, B_2^{int}, and K_2 in event-shape resummation and the corresponding constants needed for a parton shower. This holds even if the shower does not reproduce the full relevant physics at second order in the large-angle and hard-collinear regions and at third order in the soft-collinear region. This is in analogy with the fact that including the correct K_1 constant is sufficient to obtain NLL accuracy even without the real double-soft contribution.

In the next few paragraphs we will identify the relations between individual resummation and shower ingredients (neglecting terms beyond NNLL), and then show how they combine to achieve overall NNLL shower accuracy. Let us start by recalling how the $\mathcal{O}(\alpha_s^2)$ terms of Eq. (2) come about. Consider a Born squared matrix element, $\mathcal{B}_{\tilde{\imath}}$, for producing a gluon $\tilde{\imath}$ (multiplied by $\alpha_s/2\pi$). Schematically the $\mathcal{O}(\alpha_s^2)$ terms involve the single-emission virtual correction $\mathcal{V}_{\tilde{\imath}}$ and an integral over a real $\tilde{\imath} \to ij$ branching phase space and matrix element, $d\Phi_{ij|\tilde{\imath}} \mathcal{R}_{ij}$ [both multiply $(\alpha_s/2\pi)^2$]. The key difference between a resummation calculation and a parton shower lies in the phase-space mapping that is encoded in $d\Phi_{ij|\tilde{\imath}}$. For example, in many resummation calculations $g_{\tilde{\imath}} \to q_i \bar{q}_j$ splitting implicitly conserves transverse momentum $k_{t,i+j} = k_{t\tilde{\imath}}$ and rapidity $y_{i+j} = y_{\tilde{\imath}}$ with respect to the particle that emitted $\tilde{\imath}$ [58,66]. A parton shower (PS) will organize the phase space differently, and in a way that does not conserve these kinematic quantities. The difference can be represented as an effective drift in one or more kinematic variables x (e.g., $x \equiv \ln k_t$, $x \equiv y$) of post- versus prebranching kinematics. The average drifts, $(\alpha_s/2\pi)\langle \Delta_x \rangle$, are represented as arrows in Fig. 1. For a soft-collinear (SC) gluon $k_{\tilde{\imath}}$, they are independent of the kinematics of $k_{\tilde{\imath}}$. For the $C_F C_A$ and $C_F n_f$ color channels they read

$$\langle \Delta_x \rangle = \lim_{\tilde{\imath} \to \mathrm{SC}} \frac{1}{\mathcal{B}_{\tilde{\imath}}} \int d\Phi^{\mathrm{PS}}_{ij|\tilde{\imath}} \mathcal{R}_{ij} \times (x_{i+j} - x_{\tilde{\imath}}). \tag{4}$$

For the C_F^2 channel, one replaces x_{i+j} with the x value of that of i and j that corresponds to the larger shower ordering variable ($v_{\mathrm{PS}} = k_t e^{-\beta_{\mathrm{PS}}|y|}$). Note that the sign of $\langle \Delta_y \rangle$ depends on the sign of $y_{\tilde{\imath}}$ (below, $y_{\tilde{\imath}} > 0$).

To understand the relation of $\langle \Delta_y \rangle$ with $\Delta K_1^{\mathrm{int}}$, observe that a drift to large absolute rapidities depletes radiation at central rapidities. However the shower must correctly reproduce the total final amount of radiation integrated over any rapidity window. That can only be achieved with a value for $\Delta K_1^{\mathrm{int}}$ that generates just enough extra central radiation to compensate for the drift-induced depletion. Quantitatively, the following relation can be proven (Supplemental Material [72], Sec. 1)

$$\Delta K_1^{\mathrm{int,PS}} = 2\langle \Delta_y \rangle. \tag{5}$$

As a numerical check, Table I shows the result of $\Delta K_1^{\mathrm{int,PS}}$ as determined in Ref. [29], compared to $\langle \Delta_y \rangle$ as determined for this paper. The results are given for three variants [5,29] of the PanGlobal shower. The $\mathrm{PG}_{\beta=0}$ and $\mathrm{PG}^{\mathrm{sdf}}_{\beta=0}$ showers have $\beta_{\mathrm{PS}} = 0$ and differ in how the splitting probabilities are assigned between the two dipole ends. For all three variants, one observes good agreement between $\Delta K_1^{\mathrm{int,PS}}$ and $2\langle \Delta_y \rangle$.

Turning to $B_2(z)$, the corresponding physics differentially in z cannot yet be included in our showers, insofar as they lack triple-collinear splitting. However, we can use a constraint analogous to Eq. (5) to determine the correct $B_2^{\mathrm{int,PS}}$, starting from the NLO $1 \to 2$ calculations of Refs. [67,68], which conserve the light-cone momentum-fraction $z = m_t e^y = \sqrt{k_t^2 + m^2} e^y$. Specifically (Ref. [72], Sec. 2),

TABLE I. The $\Delta K_1^{\mathrm{int,PS}}$ and $\langle \Delta_y \rangle$ and $\langle \Delta_{\ln k_t} \rangle$ coefficients, including the relevant leading-N_C color factors ($2C_F = C_A = 3$ and $n_f = 5$). The errors on $\Delta K_1^{\mathrm{int,PS}}$ are systematic dominated and estimated only to within a factor of order 1. Their impact on the NNLL tests below is an order of magnitude smaller than the accuracies of those tests.

Shower	Color	$(1/4\pi)\Delta K_1^{\mathrm{int,PS}}$	$(1/2\pi)\langle \Delta_y \rangle$	$(1/2\pi)\langle \Delta_{\ln k_t} \rangle$
$\mathrm{PG}^{\mathrm{sdf}}_{\beta=0}$	C_F	0	0.000018(39)	−1.953481(1)
	C_A	0	0.000002(2)	1.162602(2)
	$n_f T_R$	0	−0.0000003(3)	−0.1048049(3)
$\mathrm{PG}_{\beta=0}$	C_F	0.04967(3)	0.049576(8)	−1.964624(6)
	C_A	0.0323(5)	0.032107(4)	1.174900(4)
	$n_f T_R$	0.0040(1)	0.003962(1)	−0.104655(1)
$\mathrm{PG}_{\beta=\frac{1}{2}}$	C_F	1.6725(5)	1.672942(9)	−1.749920(5)
	C_A	0.0172(11)	0.015303(5)	1.172042(5)
	$n_f T_R$	0.0535(2)	0.053476(1)	−0.094205(1)

$$B_2^{\mathrm{int,PS}} = B_2^{\mathrm{int,NLO}} - \langle \Delta_{\ln z} \rangle, \tag{6}$$

with

$$\langle \Delta_{\ln z} \rangle = \langle \Delta_y \rangle + \langle \Delta_{\ln m_t} \rangle = \langle \Delta_y \rangle + \langle \Delta_{\ln k_t} \rangle - \frac{\beta_0 \pi^2}{12}. \tag{7}$$

The $\beta_0 = (11C_A - 4n_f T_R)/6$ term arises from the relation between the drifts in m_t and k_t, which is shower-independent [58,66,72]. (In the C_F channel one defines the drift from the single parton with larger $k_t e^{-\beta_{\mathrm{PS}}|y|}$, so $m_t = k_t$ and $\langle \Delta_{\ln m_t} \rangle_{C_F} = \langle \Delta_{\ln k_t} \rangle_{C_F}$.) Note that Eq. (6) does not constrain the functional form of $B_2^{\mathrm{PS}}(z)$. To do so meaningfully would require a shower that incorporates triple-collinear splitting functions. For event-shape NNLL accuracy, any reasonable functional form for $B_2^{\mathrm{PS}}(z)$ is equally valid, as long as it has the correct integral. We choose the simple ansatz $B_2^{\mathrm{PS}}(z) \propto z$, normalized so as to satisfy Eq. (6). Note that in an analytical resummation, Eq. (1) would use $B_2^{\mathrm{int,resum}} = B_2^{\mathrm{int,NLO}} + (\beta_0 \pi^2/12)$ [the $(\beta_0 \pi^2/12)$ term has the same origin as in Eq. (7)].

The next ingredient that we need is K_2, which, for resummations, has been calculated in two schemes [58,66]. We adopt the scheme in which transverse momentum is conserved and consider the amount of radiation in a (fixed-rapidity) transverse-momentum window $k_{tb} < k_t < k_{ta}$, where k_t is the postbranching pair transverse momentum. The total amount of radiation in the window should be the same in the resummation and the shower. In the shower specifically, one should account for the $\ln k_t$ drifts through the lower and upper edges of the window, which involve α_s at scales k_{tb} and k_{ta} respectively. Defining $T_n(k_{tb}, k_{ta}) = \int_{k_{tb}}^{k_{ta}} (dk_t/k_t)[\alpha_s^n(k_t)/(2\pi)^n]$, that yields the constraint

$$\begin{aligned} K_2^{\mathrm{resum}} T_3(k_{tb}, k_{ta}) &= K_2^{\mathrm{PS}} T_3(k_{tb}, k_{ta}) \\ &\quad + \left(\frac{\alpha_s^2(k_{tb})}{4\pi^2} - \frac{\alpha_s^2(k_{ta})}{4\pi^2} \right) \langle \Delta_{\ln k_t} \rangle, \end{aligned} \tag{8}$$

where the second line accounts for the drift contributions at the edges. Setting

$$K_2^{\mathrm{PS}} = K_2^{\mathrm{resum}} - 4\beta_0 \langle \Delta_{\ln k_t} \rangle, \tag{9}$$

ensures Eq. (8) is satisfied for all NNLL terms $\alpha_s^{2+n} \ln^n k_{t1}/k_{t2}$, noting that for 1-loop running,

$$2n\beta_0 T_{n+1}(k_{tb}, k_{ta}) = [\alpha_s^n(k_{tb}) - \alpha_s^n(k_{ta})]/(2\pi)^n. \tag{10}$$

The final element in the connection with analytic resummation is $\mathcal{F}$, which encodes the effect of emissions near the boundary $V(k) \sim v$. The shower generates this factor through the interplay between real and virtual emission. However $\mathcal{F}^{\mathrm{PS}}$ differs from $\mathcal{F}^{\mathrm{resum}}$ because of relative drifts across the boundary (Ref. [72], Sec. 3)

$$\frac{\mathcal{F}^{\mathrm{PS}}}{\mathcal{F}^{\mathrm{resum}}} = 1 + 8C_F T_2(v, v_{\mathrm{hc}}) \left[\langle \Delta_y \rangle - \frac{1}{\beta_{\mathrm{obs}}} \langle \Delta_{\ln k_t} \rangle \right], \quad (11)$$

with $v_{\mathrm{hc}} \equiv v^{[1/(1+\beta_{\mathrm{obs}})]}$. Concentrating on the right-hand half of the Lund plane in Fig. 1, it encodes the fact that a positive y drift increases the number of events that pass the constraint $V(\{k\}) < v$, because emissions to the left of the boundary move to the right of the boundary, and vice versa for a positive $\ln k_t$ drift.

We are now in a position to write the ratio of $\Sigma(v)$ in the shower as compared to a resummation. Assembling the contributions discussed above into Eq. (1) yields

$$\begin{aligned} \frac{\Sigma^{\mathrm{PS}}(v)}{\Sigma^{\mathrm{resum}}(v)} - 1 = 8C_F \Big\{ & -\langle \Delta_y \rangle T_2(v, 1) \\ & + [\langle \Delta_y \rangle + \langle \Delta_{\ln k_t} \rangle] T_2(v_{\mathrm{hc}}, 1) \\ & + \langle \Delta_{\ln k_t} \rangle \left[\frac{1}{\beta_{\mathrm{obs}}} T_2(v, v_{\mathrm{hc}}) - T_2(v_{\mathrm{hc}}, 1) \right] \\ & + \left[\langle \Delta_y \rangle - \frac{1}{\beta_{\mathrm{obs}}} \langle \Delta_{\ln k_t} \rangle \right] T_2(v, v_{\mathrm{hc}}) \Big\} = 0, \end{aligned} \quad (12)$$

up to NNLL. The lines account, respectively, for the shower contributions to ΔK_1, B_2, K_2 [using Eq. (10) and then trading rapidity and k_t integrations] and $\mathcal{F}$. The fact that they add up to zero ensures shower NNLL accuracy for arbitrary global event shapes. The last line necessarily involves real double-soft emissions in the soft-collinear region, thus tying the other three lines (which just involve the Sudakov nonemission probability) to the shower's double-soft emissions, as anticipated below Eq. (3). The connection with the ARES NNLL formalism [51,52,58] is discussed in Ref. [72], Sec. 4.

Besides the analytic proof, we also carry out a series of numerical verifications of the NNLL accuracy of several parton showers with the above elements, using a leading-color limit $2C_F = C_A = 3$. These tests help provide confidence both in the overall picture and in our specific implementation for final-state showers. Figure 2 shows a suitably normalized logarithm of the ratio of the cumulative shower and resummed cross sections, for a specific observable, the two-to-three jet resolution parameter, y_{23}, for the Cambridge jet algorithm [73] in $Z \to q\bar{q}$ (left) and $H \to gg$ (right) processes. Focusing on the $\mathrm{PG}^{\mathrm{sdf}}_{\beta_{\mathrm{PS}}=0}$ shower, the plots show results with various subsets of ingredients. A zero result indicates NNLL accuracy. Only with 2-jet NLO matching [74], double-soft corrections [29], B_2 [67,68] terms, 3-loop running of α_s [75,76], K_2 contributions [58,66], and the drift correction of this Letter does one obtain agreement with the known NNLL predictions

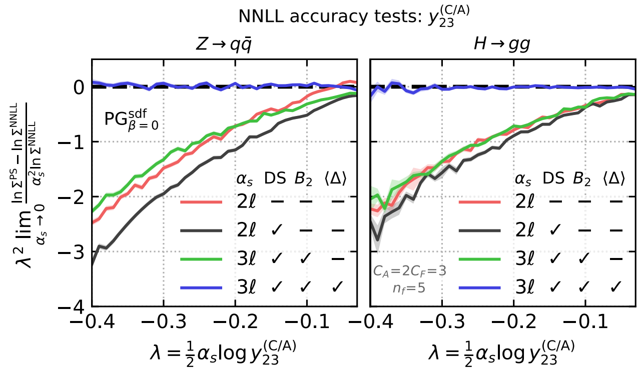

FIG. 2. Test of NNLL accuracy of the PanGlobal ($\mathrm{PG}^{\mathrm{sdf}}_{\beta=0}$) shower for the cumulative distribution of the Cambridge y_{23} resolution variable, compared to known results for $Z \to q\bar{q}$ [52] (left) and $H \to gg$ [77] (right). The curves show the difference relative to NNLL for various subsets of ingredients. Starting from the red curve, DS additionally includes double soft contributions and 2-jet NLO matching; 3ℓ includes 3-loop running of α_s and the K_2^{resum} term. B_2 in the legend refers only to its resummation part, $B_2^{\mathrm{int,NLO}}$. Including all effects (blue line) gives a result that is consistent with zero, i.e., in agreement with NNLL.

[52,77]. For this shower and observable, the drift correction dominates.

Tests across a wider range of observables and shower variants are shown in Fig. 3 for a fixed value of $\lambda = \alpha_s \ln v = -0.4$. With the drifts and all other contributions included, there is good agreement with the NNLL predictions [45–52,58,61,77].

Earlier work on NLL accuracy had found that the coefficients of NLL violations in common showers tended

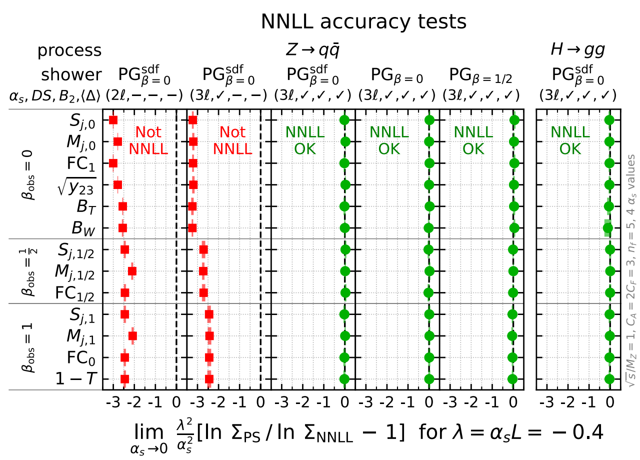

FIG. 3. Summary of NNLL tests across observables and shower variants. Results consistent with zero (shown in green) are in agreement with NNLL. The observables correspond to the event shapes used in Ref. [5] and they are grouped according to the power (β_{obs}) of their dependence on the emission angle. All showers that include the corrections of this Letter agree with NNLL.

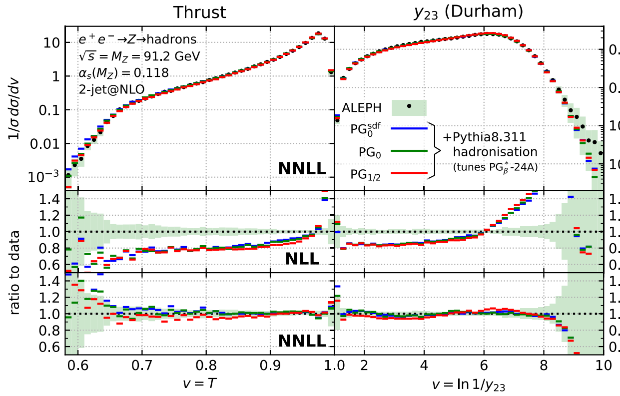

FIG. 4. Results for the Thrust and Durham y_{23} [84] observables with the PanGlobal showers compared to ALEPH data [78], using $\alpha_s(M_Z) = 0.118$. The lower (middle) panel shows the ratios of the NNLL (NLL) shower variants to data.

to be moderate for relatively inclusive observables like event shapes [5]. In contrast, here we see that non-NNLL showers differ from NNLL accuracy with coefficients of order one. That suggests a potential non-negligible phenomenological effect.

Figure 4 compares three PanGlobal showers with ALEPH data [78] using Rivet v3 [79], illustrating the showers in their NLL and NNLL variants, with $\alpha_s^{\overline{\rm MS}}(M_Z) = 0.118$ for both. We use 2-jet NLO matching [74], and the NODS color scheme [6], which guarantees full-color accuracy in terms up to NLL for global event shapes. Our showers are implemented in a pre-release of PanScales [80] v0.2.0, interfaced to Pythia v8.311 [3] for hadronization, with nonperturbative parameters tuned to ALEPH [78,81] and L3 [82] data (starting from the Monash 13 tune [83], cf. Ref. [72] Sec. 5; the tune has only a modest impact on the observables of Fig. 4). The impact of the NNLL terms is significant and brings the showers into good agreement with ALEPH data [78], both in terms of normalization and shape. Some caution is required in interpreting the results: given that the logarithms are not particularly large at LEP energies, NLO 3-jet corrections (not included) may also play a significant role and should be studied in future work. Furthermore, the PanGlobal showers do not include finite quark-mass effects. Still, Fig. 4 suggests that NNLL terms have the potential to resolve a long-standing issue in which a number of dipole showers (including notably the Pythia 8 shower, but also the PanGlobal NLL shower) required an anomalously large value of $\alpha_s(m_Z) \gtrsim 0.130$ [83] to achieve agreement with the data.

The parton showers developed here are expected to achieve NNLL (leading-color) accuracy also for nonglobal event shapes such as hemisphere or jet observables, and $\alpha_s^n L^{n-1}$ (NSL) accuracy [54,62–64,68,85,86] for the soft-drop [87,88] family of observables, in the limit where either their $z_{\rm cut}$ parameter is taken small or $\beta_{\rm SD} > 0$. (We have not carried out corresponding logarithmic-accuracy tests, because the small $z_{\rm cut}$ limit renders them somewhat more complicated than those of Figs. 2 and 3. In the case of nonglobal event shapes, there exist no reference calculations.) This is in addition to the NSL accuracy for energy flow in a slice [89–91] and $\alpha_s^n L^{2n-2}$ (NNDL) accuracy for subjet multiplicities [92] that was already achieved with the inclusion of double-soft corrections [29].

Next objectives in the programme of bringing higher logarithmic accuracy to parton showers should include incorporation of full triple-collinear splitting functions (as relevant for experimentally important observables such as fragmentation functions), the extension to initial-state radiation, and logarithmically consistent higher-order matching for a variety of hadron-collider processes. The results presented here, a significant advance in their own right, also serve to give confidence in the feasibility and value of this broad endeavor.

Acknowledgments—We are grateful to Peter Skands for discussions and helpful suggestions on nonperturbative tunes in Pythia and to Silvia Zanoli for comments on the manuscript. This work has been funded by the European Research Council (ERC) under the European Union's Horizon 2020 research and innovation programme (Grant Agreement No. 788223, M. D., K. H., J. H., G. P. S., G. S.) and under its Horizon Europe programme (Grant Agreement No. 101044599, PM), by a Royal Society Research Professorship (RP\R1\231001, G. P. S.) and by the Science and Technology Facilities Council (STFC) under Grants ST/T000864/1 (G. P. S.), ST/X000761/1 (G. P. S.), ST/T000856/1 (K. H.) and ST/X000516/1 (K. H.), ST/T001038/1 (M. D.) and ST/00077X/1 (M. D.). L. S. is supported by the Australian Research Council through a Discovery Early Career Researcher Award (Project No. DE230100867). B. K. E. is supported by the Australian Research Council via Discovery Project No. DP220103512. We also thank each others' institutes for hospitality during the course of this work.

Views and opinions expressed are those of the authors only and do not necessarily reflect those of the European Union or the European Research Council Executive Agency. Neither the European Union nor the granting authority can be held responsible for them.

[1] J. M. Campbell *et al.*, SciPost Phys. **16**, 130 (2024).
[2] E. Bothmann *et al.* (Sherpa Collaboration), SciPost Phys. **7**, 034 (2019).
[3] C. Bierlich *et al.*, SciPost Phys. Codebases **2022**, 8 (2022).
[4] G. Bewick *et al.*, Eur. Phys. J. C **84**, 1053 (2024).
[5] M. Dasgupta, F. A. Dreyer, K. Hamilton, P. F. Monni, G. P. Salam, and G. Soyez, Phys. Rev. Lett. **125**, 052002 (2020).
[6] K. Hamilton, R. Medves, G. P. Salam, L. Scyboz, and G. Soyez, J. High Energy Phys. 03 (2021) 041.

[7] A. Karlberg, G. P. Salam, L. Scyboz, and R. Verheyen, Eur. Phys. J. C **81**, 681 (2021).
[8] K. Hamilton, A. Karlberg, G. P. Salam, L. Scyboz, and R. Verheyen, J. High Energy Phys. 03 (2022) 193.
[9] M. van Beekveld, S. Ferrario Ravasio, G. P. Salam, A. Soto-Ontoso, G. Soyez, and R. Verheyen, J. High Energy Phys. 11 (2022) 019.
[10] M. van Beekveld, S. Ferrario Ravasio, K. Hamilton, G. P. Salam, A. Soto-Ontoso, G. Soyez, and R. Verheyen, J. High Energy Phys. 11 (2022) 020.
[11] M. van Beekveld and S. Ferrario Ravasio, J. High Energy Phys. 02 (2024) 001.
[12] J. R. Forshaw, J. Holguin, and S. Plätzer, J. High Energy Phys. 09 (2020) 014.
[13] Z. Nagy and D. E. Soper, arXiv:2011.04777.
[14] Z. Nagy and D. E. Soper, Phys. Rev. D **104**, 054049 (2021).
[15] F. Herren, S. Höche, F. Krauss, D. Reichelt, and M. Schoenherr, J. High Energy Phys. 10 (2023) 091.
[16] B. Assi and S. Höche, Phys. Rev. D **109**, 114008 (2024).
[17] C. T. Preuss, J. High Energy Phys. 07 (2024) 161.
[18] S. Höche, F. Krauss, and D. Reichelt, arXiv:2404.14360.
[19] S. Jadach, A. Kusina, M. Skrzypek, and M. Slawinska, J. High Energy Phys. 08 (2011) 012.
[20] L. Hartgring, E. Laenen, and P. Skands, J. High Energy Phys. 10 (2013) 127.
[21] S. Jadach, A. Kusina, W. Płaczek, and M. Skrzypek, Acta Phys. Pol. B **44**, 2179 (2013).
[22] S. Jadach, A. Kusina, W. Placzek, and M. Skrzypek, J. High Energy Phys. 08 (2016) 092.
[23] H. T. Li and P. Skands, Phys. Lett. B **771**, 59 (2017).
[24] S. Höche and S. Prestel, Phys. Rev. D **96**, 074017 (2017).
[25] S. Höche, F. Krauss, and S. Prestel, J. High Energy Phys. 10 (2017) 093.
[26] F. Dulat, S. Hoeche, and S. Prestel, Phys. Rev. D **98**, 074013 (2018).
[27] J. M. Campbell, S. Höche, H. T. Li, C. T. Preuss, and P. Skands, Phys. Lett. B **836**, 137614 (2023).
[28] L. Gellersen, S. Höche, and S. Prestel, Phys. Rev. D **105**, 114012 (2022).
[29] S. Ferrario Ravasio, K. Hamilton, A. Karlberg, G. P. Salam, L. Scyboz, and G. Soyez, Phys. Rev. Lett. **131**, 161906 (2023).
[30] Z. Nagy and D. E. Soper, J. High Energy Phys. 07 (2015) 119.
[31] Z. Nagy and D. E. Soper, Phys. Rev. D **99**, 054009 (2019).
[32] Z. Nagy and D. E. Soper, Phys. Rev. D **100**, 074005 (2019).
[33] M. De Angelis, J. R. Forshaw, and S. Plätzer, Phys. Rev. Lett. **126**, 112001 (2021).
[34] J. Holguin, J. R. Forshaw, and S. Plätzer, Eur. Phys. J. C **81**, 364 (2021).
[35] S. Höche and D. Reichelt, Phys. Rev. D **104**, 034006 (2021).
[36] Y. Hatta and T. Ueda, Nucl. Phys. **B874**, 808 (2013).
[37] Y. Hagiwara, Y. Hatta, and T. Ueda, Phys. Lett. B **756**, 254 (2016).
[38] Y. Hatta and T. Ueda, Nucl. Phys. **B962**, 115273 (2021).
[39] T. Becher, M. Neubert, and D. Y. Shao, Phys. Rev. Lett. **127**, 212002 (2021).
[40] T. Becher, M. Neubert, D. Y. Shao, and M. Stillger, J. High Energy Phys. 12 (2023) 116.
[41] P. Böer, P. Hager, M. Neubert, M. Stillger, and X. Xu, J. High Energy Phys. 08 (2024) 035.
[42] S. Brandt, C. Peyrou, R. Sosnowski, and A. Wroblewski, Phys. Lett. **12**, 57 (1964).
[43] E. Farhi, Phys. Rev. Lett. **39**, 1587 (1977).
[44] D. de Florian and M. Grazzini, Nucl. Phys. **B704**, 387 (2005).
[45] T. Becher and M. D. Schwartz, J. High Energy Phys. 07 (2008) 034.
[46] R. Abbate, M. Fickinger, A. H. Hoang, V. Mateu, and I. W. Stewart, Phys. Rev. D **83**, 074021 (2011).
[47] Y.-T. Chien and M. D. Schwartz, J. High Energy Phys. 08 (2010) 058.
[48] P. F. Monni, T. Gehrmann, and G. Luisoni, J. High Energy Phys. 08 (2011) 010.
[49] T. Becher and G. Bell, J. High Energy Phys. 11 (2012) 126.
[50] A. H. Hoang, D. W. Kolodrubetz, V. Mateu, and I. W. Stewart, Phys. Rev. D **91**, 094017 (2015).
[51] A. Banfi, H. McAslan, P. F. Monni, and G. Zanderighi, J. High Energy Phys. 05 (2015) 102.
[52] A. Banfi, H. McAslan, P. F. Monni, and G. Zanderighi, Phys. Rev. Lett. **117**, 172001 (2016).
[53] C. Frye, A. J. Larkoski, M. D. Schwartz, and K. Yan, arXiv:1603.06375.
[54] C. Frye, A. J. Larkoski, M. D. Schwartz, and K. Yan, J. High Energy Phys. 07 (2016) 064.
[55] Z. Tulipánt, A. Kardos, and G. Somogyi, Eur. Phys. J. C **77**, 749 (2017).
[56] I. Moult and H. X. Zhu, J. High Energy Phys. 08 (2018) 160.
[57] G. Bell, A. Hornig, C. Lee, and J. Talbert, J. High Energy Phys. 01 (2019) 147.
[58] A. Banfi, B. K. El-Menoufi, and P. F. Monni, J. High Energy Phys. 01 (2019) 083.
[59] M. Procura, W. J. Waalewijn, and L. Zeune, J. High Energy Phys. 10 (2018) 098.
[60] L. Arpino, A. Banfi, and B. K. El-Menoufi, J. High Energy Phys. 07 (2020) 171.
[61] C. W. Bauer, A. V. Manohar, and P. F. Monni, J. High Energy Phys. 07 (2021) 214.
[62] A. Kardos, A. J. Larkoski, and Z. Trócsányi, Phys. Lett. B **809**, 135704 (2020).
[63] D. Anderle, M. Dasgupta, B. K. El-Menoufi, J. Helliwell, and M. Guzzi, Eur. Phys. J. C **80**, 827 (2020).
[64] M. Dasgupta, B. K. El-Menoufi, and J. Helliwell, J. High Energy Phys. 01 (2023) 045.
[65] C. Duhr, B. Mistlberger, and G. Vita, Phys. Rev. Lett. **129**, 162001 (2022).
[66] S. Catani, D. De Florian, and M. Grazzini, Eur. Phys. J. C **79**, 685 (2019).
[67] M. Dasgupta and B. K. El-Menoufi, J. High Energy Phys. 12 (2021) 158.
[68] M. van Beekveld, M. Dasgupta, B. K. El-Menoufi, J. Helliwell, and P. F. Monni, J. High Energy Phys. 05 (2024) 093.
[69] A. Banfi, G. P. Salam, and G. Zanderighi, J. High Energy Phys. 03 (2005) 073.
[70] B. Andersson, G. Gustafson, L. Lonnblad, and U. Pettersson, Z. Phys. C **43**, 625 (1989).

[71] S. Catani, B. R. Webber, and G. Marchesini, Nucl. Phys. **B349**, 635 (1991).

[72] See Supplemental Material at http://link.aps.org/supplemental/10.1103/PhysRevLett.134.011901 for details on analytic ingredients and tuning.

[73] Y. L. Dokshitzer, G. D. Leder, S. Moretti, and B. R. Webber, J. High Energy Phys. 08 (1997) 001.

[74] K. Hamilton, A. Karlberg, G. P. Salam, L. Scyboz, and R. Verheyen, J. High Energy Phys. 03 (2023) 224.

[75] O. V. Tarasov, A. A. Vladimirov, and A. Y. Zharkov, Phys. Lett. **93B**, 429 (1980).

[76] S. A. Larin and J. A. M. Vermaseren, Phys. Lett. B **303**, 334 (1993).

[77] M. van Beekveld, L. Buonocore, B. El-Menoufi, S. Ferrario Ravasio, P. Monni, A. Soto-Ontoso, and G. Soyez (to be published).

[78] A. Heister *et al.* (ALEPH Collaboration), Eur. Phys. J. C **35**, 457 (2004).

[79] C. Bierlich *et al.*, SciPost Phys. **8**, 026 (2020).

[80] M. van Beekveld *et al.*, SciPost Phys. Codebases **2024**, 31 (2024).

[81] R. Barate *et al.* (ALEPH Collaboration), Phys. Rep. **294**, 1 (1998).

[82] P. Achard *et al.* (L3 Collaboration), Phys. Rep. **399**, 71 (2004).

[83] P. Skands, S. Carrazza, and J. Rojo, Eur. Phys. J. C **74**, 3024 (2014).

[84] S. Catani, Y. L. Dokshitzer, M. Olsson, G. Turnock, and B. R. Webber, Phys. Lett. B **269**, 432 (1991).

[85] Z.-B. Kang, K. Lee, X. Liu, and F. Ringer, Phys. Lett. B **793**, 41 (2019).

[86] G. Bell, R. Rahn, and J. Talbert, J. High Energy Phys. 09 (2020) 015.

[87] M. Dasgupta, A. Fregoso, S. Marzani, and G. P. Salam, J. High Energy Phys. 09 (2013) 029.

[88] A. J. Larkoski, S. Marzani, G. Soyez, and J. Thaler, J. High Energy Phys. 05 (2014) 146.

[89] A. Banfi, F. A. Dreyer, and P. F. Monni, J. High Energy Phys. 10 (2021) 006.

[90] A. Banfi, F. A. Dreyer, and P. F. Monni, J. High Energy Phys. 03 (2022) 135.

[91] T. Becher, N. Schalch, and X. Xu, Phys. Rev. Lett. **132**, 081602 (2024).

[92] R. Medves, A. Soto-Ontoso, and G. Soyez, J. High Energy Phys. 10 (2022) 156.